

Elastic Strain Measurement of Miniature Tensile Specimens

F. Hajy Akbary · M.J. Santofimia · J. Sietsma

Received: 1 November 2012 / Accepted: 8 July 2013 / Published online: 6 August 2013
© Society for Experimental Mechanics 2013

Abstract The measurement of elastic strain in miniature specimens by means of the crosshead displacement recorded with a tensile-test machine is influenced by the elongation of the two fillet-zones and the compliance of the testing device. In this paper, a mathematical model for calculating the elastic elongation of the fillet-zones of a dog-bone tensile specimen and the machine compliance as a function of the applied load is proposed. The subtraction of the fillet-zones elongation and the machine compliance from the crosshead displacement allows the calculation of the elastic elongation of miniature specimens leading to values in agreement with strains measured via digital image correlation.

Keywords Miniature specimen · Crosshead displacement · Fillet-zones · Machine compliance

Introduction

Nowadays, the development of new fabrication technologies and miniaturized products which restrict the specimen dimensions results in an increased use of miniaturized tests for studying mechanical properties of materials. Additionally, analysing miniature specimens instead of standard ones saves material and time for both industrial and academic researchers.

Generally, tensile specimens used in miniaturized tests are dog-bone shaped. A dog-bone tensile specimen can be divided into five zones: the parallel-zone, the two fillet-zones and

the two grip-zones (Fig. 1). Dimensions of miniature specimens deviate from ASTM standards, the parallel length of miniature specimens being in the range from 1 mm [1] to several millimetres [2, 3].

The knowledge of the elastic properties of materials, e. g. elastic strain and stress, is important for engineering design processes. Although the elastic stress of miniature specimens can be accurately calculated from the force that is recorded by the tensile-test machine, measuring the precise elastic strain is challenging. The elastic strain of standard specimens can be accurately determined by using clip-on extensometers, but this option is difficult in miniature specimens due to their small dimensions [4]. At present, there exist non-contacting strain measuring systems such as laser and video extensometers [5] but their high price and complex set-up limit their application. Therefore, using extensometer is not a common method for elastic strain measurements of miniature specimens.

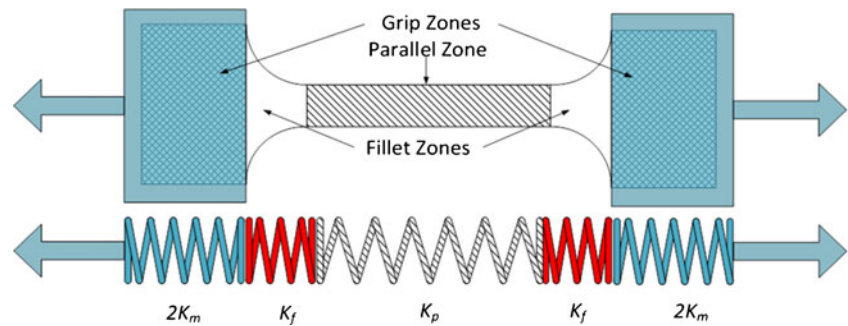
There are two main alternatives to the use of extensometers for determining the elastic strain of miniature specimens: the application of Digital Image Correlation (DIC) and the measurement of the strain from the crosshead displacement that is recorded by the tensile-test machine. The DIC method consists of the measurement of the strain of the specimen during testing by comparing, pixel by pixel, images of the specimen before and after elongation. This technique requires the use of a high resolution camera, followed by data post-processing by using the corresponding software. On the other hand, the measurement of the elastic strain of miniature specimens from the crosshead displacement does not need any extra equipment and data processing. However, one drawback of using crosshead displacement for elastic strain measurements, is that the elongation of the fillet-zones of the specimen and the tensile machine parts are included in the crosshead displacement. Therefore, this method overestimates the elastic strain of miniature specimens, as will be detailed further on.

Although elongation of the fillet-zones of miniature specimens during tensile tests has been reported by different

F. Hajy Akbary (✉)
Materials innovation institute (M2i) and Department of Materials
Science and Engineering, Delft University of Technology, 2628
CD Delft, The Netherlands
e-mail: f.hajyakbary@tudelft.nl

M.J. Santofimia · J. Sietsma
Department of Materials Science and Engineering, Delft University
of Technology, 2628 CD Delft, The Netherlands

Fig. 1 Scheme of a tensile-test machine and a dog-bone specimen which are modelled by five series of springs



researchers [6], most of the published investigations considered the fillet-zones as rigid items when measuring the strain from the crosshead displacement [7]. To eliminate the influence of the fillet-zones elongation on the measured elastic strain, Koubaa et al. [8] defined the initial length in the strain calculation as the total length of the parallel-zone and the two fillet-zones. The strain measured by their proposed approach is in better agreement with the strain calculated using finite element analysis than the strain measured by dividing the crosshead displacement by the initial length of the parallel-zone. However, their proposed method underestimates the strain, since the strain in the fillet-zones is smaller than in the parallel-zone.

A tensile-test machine is not a monolithic part and it consists of different parts like the machine frame together with measuring and fixturing devices. The machine components are not rigid and they deform elastically in tension. These elongations, which are known as machine compliance, are included in the recorded crosshead displacement [9]. The elastic elongation of miniature specimens is relatively small and the machine compliance has significant effect on the crosshead displacement. Therefore, the machine compliance should be precisely considered when the elastic strain of miniature specimens is to be measured from the crosshead displacement. The ASTM standard for tensile testing of single filament materials determines the machine compliance by assuming the tensile-test machine and specimen as two linear springs which are connected in series [10]. According to this standard, the machine stiffness depends on the specimen stiffness and dimensions. However, experimental measurements of the machine stiffness reveal that the machine stiffness is a function of the applied load and it is independent of the specimen properties [11].

The present paper establishes a new method to determine the elastic strain of miniature specimens from the crosshead displacement, based on the calculation of the fillet-zones elastic elongation and the machine compliance. The proposed model for calculating the fillet-zones elastic elongation is validated by finite element analysis. A correction method is developed to subtract the influence of the fillet-zones elastic elongation and the machine compliance from the recorded crosshead displacement. This correction method is used to

calculate the elastic strain in the parallel-zone of miniature specimens of four different steels. Resulting values are in good agreement with the elastic strains measured from DIC method.

Mathematical Modelling of the Effective Parameters on the Crosshead Displacement

A tensile-test system consists of tensile specimen and tensile-test machine. The elastic elongation of the tensile-test system components during the tensile test can be considered as the elongation of a series of springs. In this paper, the tensile test system is modelled by five springs in series: two for the tensile-test machine, two for the fillet-zones and one for the parallel-zone of the tensile specimen (Fig. 1).

In the current approach, each arm of the tensile-test machine is modelled by a spring with stiffness of $2K_m$. A factor 2 is included to simplify the calculation procedure so the total stiffness of the tensile-test machine can be considered as a single spring with stiffness K_m . The apparent stiffness that is displayed by the tensile-test system (K_{app}) is calculated as:

$$\frac{1}{K_{app}} = \frac{1}{K_m} + \frac{1}{K_p} + \frac{2}{K_f} \quad (1)$$

where K_p and K_f are the stiffness of the parallel-zone and the stiffness of one fillet of the fillet-zones of the tensile specimen, respectively. The total elongation of the tensile-test system is recorded as crosshead displacement by the tensile-test machine. This recorded displacement is defined here as the apparent elongation of the tensile specimen (Δl_{app}) and it can be calculated by:

$$\Delta l_{app} = \Delta l_m + \Delta l_p + 2\Delta l_f \quad (2)$$

where Δl_m , Δl_p and Δl_f are the elongation of the tensile-test machine parts, the elongation of the parallel-zone and the elongation of one fillet of the fillet-zones of the tensile specimen, respectively.

Elastic Elongation of the Fillet-Zones

In this section, a model is developed to calculate elastic elongation of the fillet-zones. It is known that the elastic strain can be calculated from the Hooke's Law:

$$\varepsilon = \frac{\sigma}{E} \quad (3)$$

where ε , σ and E are the elastic strain, the elastic stress and the Young's modulus of the material, respectively. The elastic strain of one fillet of the fillet-zones (ε_f) at location x , which is the distance between the boundary of the grip-zone and the fillet-zone (Fig. 2), is determined as:

$$\varepsilon_f = \frac{F}{Edw_f(x)} \quad (4)$$

where F and d are the applied force and the specimen thickness, respectively. Here, $w_f(x)$ is the specimen width in the fillet-zone as a function of x . The function $w_f(x)$ is defined as:

$$w_f(x) = w_g - 2\sqrt{r^2 - (r-x)^2} \quad (5)$$

where w_g is the specimen width at the boundary of the fillet-zone and the grip-zone and r is the fillet-zone radius. Elongation of a fillet-zone is determined as:

$$\Delta l_f = \int_0^r \varepsilon_f dx \quad (6)$$

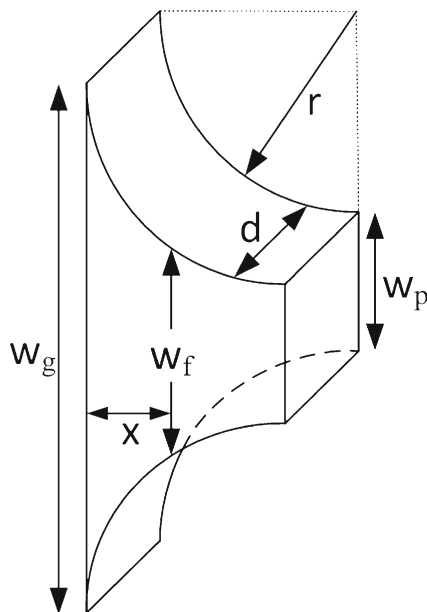


Fig. 2 Scheme of a fillet-zone of a dog-bone tensile specimen

Thereupon, elongation of a fillet-zone is calculated by substituting equations (4) and (5) into equation (6), as:

$$\Delta l_f = \int_0^r \frac{F}{Ed} \times \frac{dx}{w_g - 2\sqrt{r^2 - (r-x)^2}} \quad (7)$$

The ratio of the elongation of a fillet-zone to the elongation of the parallel-zone is:

$$\frac{\Delta l_f}{\Delta l_p} = \frac{\int_0^r \frac{dx}{w_g - 2\sqrt{r^2 - (r-x)^2}}}{\frac{l_p}{w_p}} = \alpha \quad (8)$$

where w_p and l_p are the width and the length of the specimen in the parallel-zone, respectively. The parameter α is a geometrical coefficient and it is independent of the applied force and the material.

Machine Compliance

Elastic elongation of components of a tensile-test machine during the tensile test can be modelled by the elongation of a spring with stiffness K_m . It is well established that the stiffness of a tensile-test machine (K_m) is a non-linear function of the applied force and it is independent of the specimen type and geometry [11]. The machine compliance (Δl_m) is defined by the Hooke's Law as:

$$\Delta l_m = \frac{F}{K_m} \quad (9)$$

where F is the applied force. Since K_m is a function of the applied load, it can be concluded from equation (9) that the compliance of a tensile-test machine is a function of the applied load. The compliance function is invariant for different specimens and it can be used to calculate the machine compliance at a certain value of the applied force.

Method to Calculate the Parallel-Zone Strain

The elastic elongation of the parallel-zone can be calculated from the crosshead displacement by taking the following steps:

- The first step is specifying the machine compliance function. In this matter, a specimen is tested by the tensile-test machine while the reference elongation through its parallel-zone, Δl_p^{ref} , is recorded by a direct method such as DIC. The machine compliance, at a certain value of force, is calculated by combining equations (2) and (8) and substituting the corresponding values of the

crosshead displacement (Δl_{app}) and the reference elongation (Δl_p^{ref}) in:

$$\Delta l_m = \Delta l_{app} - (1 + 2\alpha) \Delta l_p^{ref} \quad (10)$$

The geometrical coefficient, α , is computed by considering the specimen dimensions in equation (8). Finally, the compliance function (Δl_m) of the tensile-test machine is determined by plotting the machine compliance-force (Δl_m vs. F) diagram.

- b) Then, the corrected elongation of the parallel-zone (Δl_p^c) for every tensile specimen at a certain value of the applied load and apparent elongation is determined by combining equation (2) and equation (8) and substituting the machine compliance function in the following equation:

$$\Delta l_p^c = \frac{1}{(1 + 2\alpha)} (\Delta l_{app} - \Delta l_m) \quad (11)$$

The corrected elastic strain within the parallel-zone of miniature specimens (ε_p^c) is expressed as:

$$\varepsilon_p^c = \frac{1}{(1 + 2\alpha)} \left(\frac{\Delta l_{app} - \Delta l_m}{l_p} \right) \quad (12)$$

Equation (12) is independent of the material type and it can be determined for every tensile specimen at a certain value of the applied load and apparent elongation.

Method

In this paper, the elastic elongation of the miniature specimens with two different geometries and the standard specimens were investigated. According to Table 1, in the naming of the miniature specimens, T refers to the *tensile specimen* and the next digit shows the specimen parallel length in millimeter. The effect of the specimen dimensions on the elastic elongation was studied by analyzing the elastic strain measurement of the T.4 miniature specimens, via DIC, and the standard

Table 1 Nominal dimensions of the standard and miniature specimens (mm)

Specimen	Width	Thickness	Parallel length	Grip area	Overall length	Fillet radius
T.120	20.0	1.0	120.0	30.0×40.0	230.0	15.0
T.4	1.0	1.0	4.0	4.0×2.0	10.0	1.0
T.3	0.8	0.8	3.0	3.5×3.0	10.0	0.5

specimens of four different steels: viz. one interstitial free steel (IF), two dual phase steels with different fractions of ferrite (DP1000 and DP600) and one martensitic steel (M1400). A mathematical model was developed to correct the elastic strain of the miniature specimens, based on the elastic strain measurement of the T.4 miniature specimens from steel M1400. This model includes the subtraction of the fillet-zones elongation and the machine compliance from the crosshead displacement. The proposed correction method was experimentally validated with T.4 miniature specimens from different types of steels (DP1000, DP600 and IF) and T.3 miniature specimens from DP1000. The key points of the experimental procedure are given in this section.

Specimens Geometry

The dimensions of the miniature and standard tensile specimens are listed in Table 1. The specimen's axis was perpendicular to the rolling direction. The dimensions of the miniature specimens satisfied some of the ASTM standard requirements. The standard indicates that the ratio of the parallel length to the parallel width is 4 and radius of the fillet-zone is equal or greater than the width of the parallel-zone [12]. Also, to ensure that the specimen failure will occur within the parallel-zone, the standard specifies a ratio of the grip width to the parallel width equal or higher than 1.5 [13]. Miniature specimens were machined from sheets using an electro discharge machine.

Tensile Testing

For each type of material and geometry, three specimens were tested in tension. All the standard and miniaturized tensile tests were done until failure. Standard specimens were tested with a "Schenk Trebel tensile-test machine". A uniform elongation region with initial length of 80 mm was considered as the gauge length of the standard specimens. The strain of the standard specimens (ε_p^s), within the gauge length, was measured using a contact extensometer.

Miniaturized tensile tests were performed using a "Deben Microtest 5000 N Tensile Stage". For these miniaturized tests, the apparent strain (ε_{app}) was determined by dividing the recorded crosshead displacement by the initial length of the parallel-zone the specimen. Furthermore, the reference elastic strain (ε_p^{ref}) of the miniature specimens was measured by DIC technique. Before the tensile test, the flat surfaces of the miniature specimens were ground using 1200 grit SiC papers.

The engineering strain–stress curves of the standard and miniaturized tests, from zero to failure, of all the steels were presented in a previous work of the present authors [14]. Since the present research is focused on the elastic elongation of the miniature specimens, only the elastic part of the strain–stress

curves were presented in this paper. For clarity, in this work the average of the measured elastic strain and stress data were used to develop the elastic strain–stress curve.

The apparent strain rate of the standard and miniaturized tests were calculated by dividing the crosshead velocity by the initial length of the parallel-zone of the specimen. The standard and miniaturized tensile tests were performed at apparent strain rate of $2 \times 10^{-3} \text{ s}^{-1}$ at room temperature with the exception of the IF T.4 miniature specimens, which were tested at apparent strain rate of $4 \times 10^{-5} \text{ s}^{-1}$. The reason of testing the IF miniature specimens at lower strain rate was that its limited elastic elongation occurred in a few seconds. On the other hand, the DIC method requires that a camera makes consecutive images of the deforming specimen in a certain time interval, which was 6 s in the current research. Therefore, in the case of IF miniature specimens a lower strain rate is required to take an adequate number of images for accurate determination of the elastic strain.

Digital Image Correlation

The Digital Image Correlation (DIC) method was applied for measuring the elastic strain of the T.4 miniature specimens within the parallel-zone. DIC is an optical method that determines the elongation of an object during the mechanical tests. With this technique a mathematical correlation analysis is used to calculate the strain of the specimen from a series of consecutive digital images of the specimen surface [15]. To obtain accurate results with the DIC, the specimen needs to have a recognizable spackle pattern on its surface.

In this research, to guarantee a proper spackle pattern, the specimen surface was painted with a white spray and then a random black pattern was finely created with a black spray. An Oxford camera recorded images from the full parallel-zone with a resolution of $1,024 \times 768$ pixels. Finally, the “digital image correlation and tracking” toolbox of the MATLAB code was used for strain calculations. The accuracy of the DIC technique for determining strain depends on the minimum detectable displacement, which is the spatial size of a pixel in an image. The spatial size of a pixel can be calculated by dividing the specimen dimension to the camera resolution [16]. In this study, the minimum displacement that can be characterized for the T.4 miniature specimens was given by dividing the parallel length of the specimen (4 mm) by the vertical resolution of the image (1024), leading to 4×10^{-3} mm. By using this method, the minimum detectable displacement for T.3 miniature specimens was 3×10^{-3} mm. Therefore, the detection strain limit of the DIC for T.4 and T.3 miniature specimens was 10^{-3} (mm/mm) and only strains in the range from 10^{-3} (mm/mm) to the yield point were determined by the DIC technique.

Finite Element Modeling

The proposed model for calculating the elastic elongation of one fillet of the fillet-zones (equation (7)) was validated by finite element simulation of the elastic elongation of a fillet-zone. Finite element simulations were done using the commercial code ABAQUS 11.6-1. A 3D model of one fillet of the fillet-zones of the T.4 miniature specimen was developed. The elastic properties of the material in the simulation were taken from the measurement performed on the M1400 standard specimens, with Young’s modulus and the Poisson’s ratio of 210 GPa and 0.3, respectively. The fillet-zone was modeled by solid element C3D8R which is an 8-node linear brick with reduced integration and hourglass control. As it is shown in Fig. 3(a), to simulate the tensile test, the left side of the fillet-zone was encastered while the right side of the fillet was elongated. The fillet-zone was elongated by 0.02 mm. This is equal to the elongation of the parallel-zone of the T.4 miniature specimen when it was deformed by the elastic strain limit (0.005 (mm/mm)) of the M1400 standard specimen.

Results and Discussion

Results on the calculation of the elastic strain based on the proposed model and verification of this methodology are presented and discussed in this section.

Experimental Measurement of the Elastic Strain

The elastic strain–stress ($\varepsilon_p^s - \sigma$) graphs of the standard and the apparent elastic strain–stress ($\varepsilon_{app} - \sigma$) graphs of the miniature specimens for steels M1400, DP1000, DP600 and IF are illustrated in Fig. 4(a–e). Additionally, Fig. 4 presents the reference elastic strain–stress ($\varepsilon_p^{ref} - \sigma$) curves of the miniature specimens that were measured by DIC.

Figure 4(a–e) show that the reference elastic strain–stress curves of the miniature specimens and the elastic strain–stress of the standard specimens are in excellent agreement. This confirms that the specimen geometry has no significant effect on the actual measured elastic elongation of material and the elastic slope of the standard and reference miniaturized tests is independent of the specimen geometry. Furthermore, the apparent elastic slope of the miniaturized tests, which were determined from apparent elastic strain–stress ($\varepsilon_{app} - \sigma$) graphs, are lower than the standard ones. This indicates that the fillet-zones elongation and machine compliance strongly increase the crosshead displacement within the miniaturized tests.

Fig. 3 **a** 3D model of the one fillet of the fillet-zones with the applied boundary conditions and **b** the elastic elongation distributions in the fillet-zone (elongation scale is in mm)

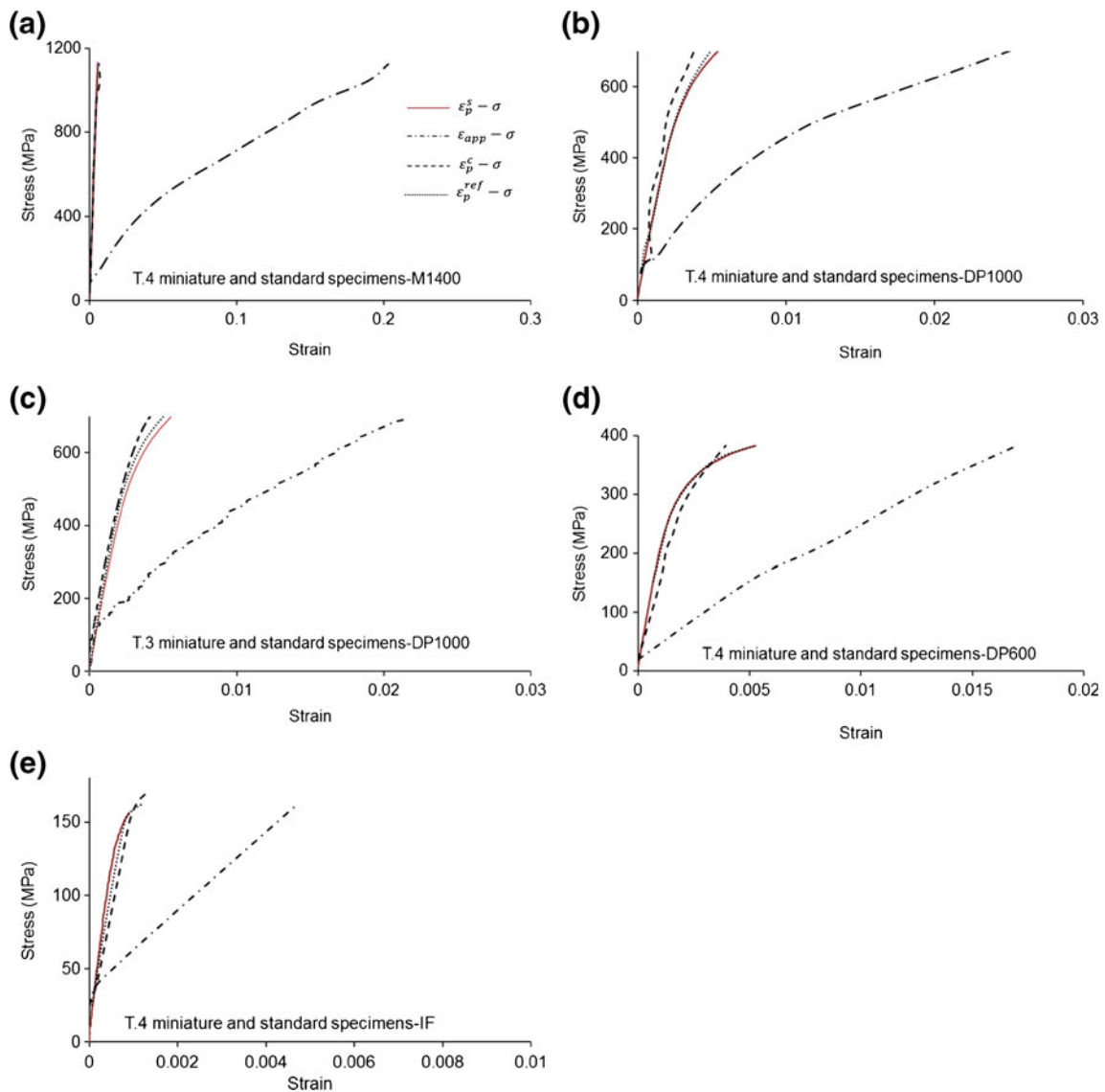
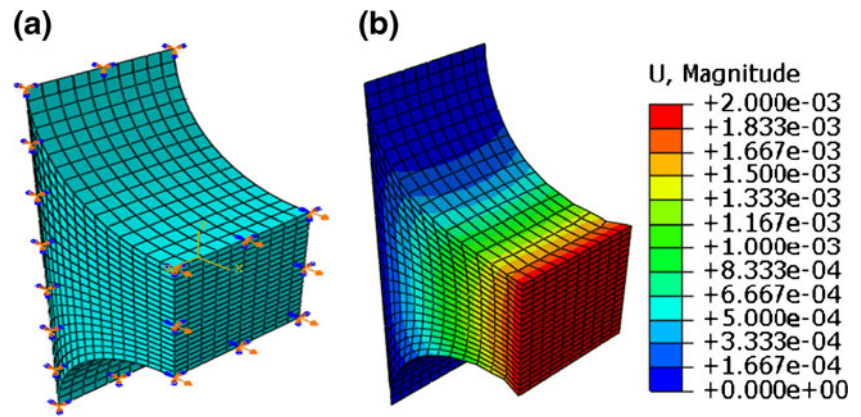


Fig. 4 Elastic strain–stress curves of **a** M1400 (standard and T.4 miniature specimens), **b** DP1000 (standard and T.4 miniature specimens), **c** DP1000 (standard and T.3 miniature specimens), **d** DP600 (standard and T.4 miniature specimens) and **e** IF (standard and T.4 miniature specimens) steels. The apparent elastic strain (ε_{app}), the reference elastic strain (ε_p^{ref}) and the corrected elastic strain (ε_p^c) of the miniature specimens were determined from the crosshead displacement, DIC and the proposed method, respectively. The elastic strain of the standard specimens (ε_p^s) was determined by extensometer

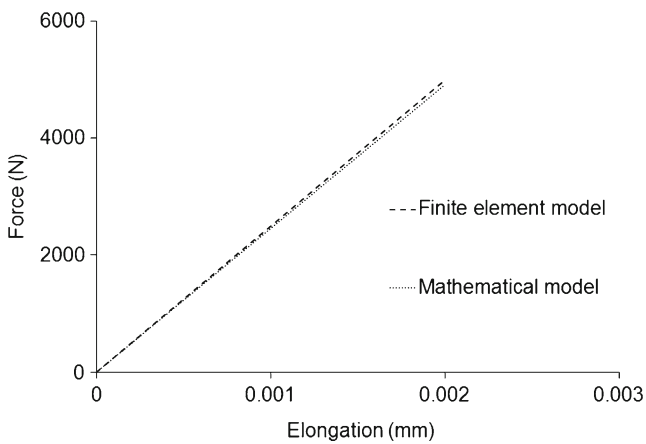


Fig. 5 The elongation-force curves of the one fillet of the fillet-zones of T.4 miniature specimen from steel M1400 calculated by FEM (dashed line) and equation (7) (dotted line)

Calculation of the Fillet-Zones Elongation and the Machine Compliance

To evaluate the accuracy of the model developed in the Section “Elastic Elongation of the Fillet-Zones”, the elastic elongation of one fillet (Δl_f) of the fillet-zones of the T.4 miniature specimen from M1400 was simulated by finite element analysis. The distribution of the elastic elongation in the fillet-zone is shown in Fig. 3(b) and it indicates that the elastic strain is not uniform in this zone, contrary to the assumption of the uniform elongation in the parallel-zone and the fillet-zones which was done by Koubaa et al. [8]. The elongation of the fillet-zone was computed from the finite element simulation and the proposed model (equation (7)) and the results of the both calculations are illustrated as the force-elastic elongation curves in Fig. 5. The results show that the proposed mathematical model calculates the fillet elongation accurately.

Substituting the T.4 miniature specimens dimensions from Table 1 in equation (8), the parameter α is found to be equal to 0.19 for these specimens. Furthermore, the ratio between the elastic elongation of one fillet of the fillet-zones and the parallel-

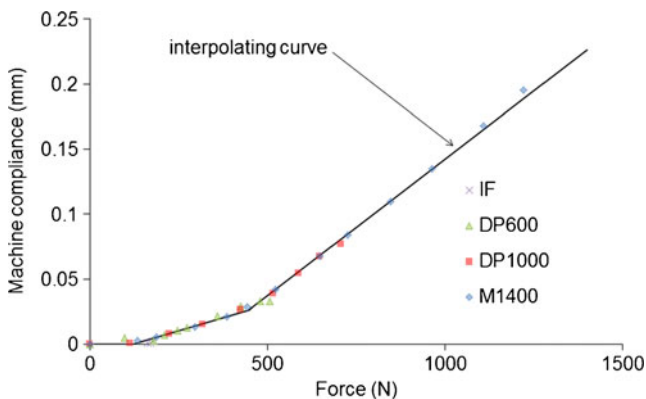


Fig. 6 Applied force-machine compliance curve of the T.4 miniature specimens from IF, DP600, DP1000 and M1400. The solid line is interpolating of the M1400 miniature specimen data

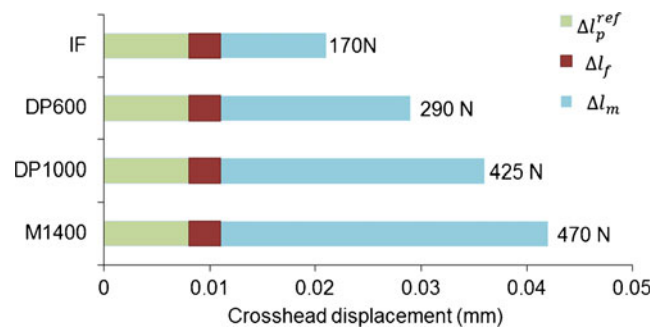


Fig. 7 Contribution of the parallel-zone elongation (Δl_p^{ref}), the fillet-zones elongation ($2\Delta l_f$) and machine compliance (Δl_m) on the crosshead displacement in the tensile testing of the T.4 miniature specimens. The parallel-zone elongation of all the steels was the same (2×10^{-3} mm) and the applied forces to create this elongation were recorded

zone was determined for the standard specimens as $\alpha=0.09$. The low value of α for the standard specimens in comparison to $\alpha=0.19$ for the T.4 miniature specimens shows that the fillet-zones elongation has a much smaller effect on the crosshead displacement of the standard specimens.

For the T.4 miniature specimens from all four groups of steels, the reference elongation of the parallel-zone (Δl_p^{ref}) was measured by DIC. The machine compliance, at different levels of Δl_p^{ref} , can be determined by using equation (10) and subtracting the elastic elongation of the fillet-zones and parallel-zone of the specimen from the crosshead displacement. The machine compliance vs. applied force diagram is illustrated in Fig. 6. This figure shows that for all the tested steels variations of the machine compliance versus the applied force follows the same trend and it is independent of the material type. By interpolation of the T.4 miniature specimen from M1400 data, the compliance function of the tensile-test machine was expressed as a bilinear curve by:

$$\Delta l_m = \begin{cases} 0 & F < 150 \text{ N} \\ 8.1 \times 10^{-5} \left(\frac{\text{mm}}{\text{N}}\right) F - 0.0096(\text{mm}) & 150 \leq F < 450 \text{ N} \\ 2.1 \times 10^{-4} \left(\frac{\text{mm}}{\text{N}}\right) F - 0.0678(\text{mm}) & 450 \leq F < 1200 \text{ N} \end{cases} \quad (13)$$

Table 2 Apparent elastic slope (E^{app}), reference elastic slope (E^{ref}) and corrected elastic slope (E^c) of the miniature specimens and elastic slope of the standard specimens (E^s). The relative error of apparent elastic slope (η^{app}) and corrected elastic slope (η^c) were calculated based on the elastic slope of the standard specimens. In this table, the elastic slope and relative error are given in GPa and percentage, respectively

Specimen	E^s	E^{ref}	E^{app}	η^{app}	E^c	η^c
T.4 M1400	203	204	55	73	204	0.5
T.4 DP1000	212	212	51	76	235	10
T.3 DP1000	212	215	50	76	220	4
T.4 DP600	202	200	98	52	187	7
T.4 IF	173	188	88	96	165	5

For forces lower than 150 N, the machine compliance is insignificant and its value is assumed zero.

For all the studied steels, the contributions of the fillet-zones elongation and the machine compliance to the crosshead displacement of one T.4 miniature specimen are illustrated in Fig. 7. In this figure, the elongation of the parallel-zone was determined by using DIC method and its value is equivalent (2×10^{-3} mm) for all the specimens. Also, the elastic elongation of the fillet-zones and the machine compliance were determined by using equations (7) and (10), respectively. Figure 7 shows that the elongation of the fillet-zones is equivalent for all the steels and as it was discussed in the Section “Elastic Elongation of the Fillet-Zones”, the ratio of the elongation of the one fillet of the fillet-zones to the elongation of the parallel-zone is independent of the material type. It can be recognized that stronger specimens deform elastically up to a higher load and thereby the machine compliance, which is function of the applied force, is larger for these specimens. This figure also indicates that, for all the steels, the machine compliance forms the main contribution on the crosshead displacement and its influence on the elastic strain measurement should be precisely considered.

Validation of the Proposed Model

The correction procedure to calculate the elastic strain in the parallel-zone of the miniature specimens was developed by inserting the machine compliance function (equation (13)) and the α value, 0.19 for the T.4 miniature specimens and 0.14 for the T.3 miniature specimen, in equation (12). Then the parallel-zone strain of the miniature specimens at different levels of the crosshead displacement and the applied force were calculated. As it can be seen in Fig. 4(a–e) the corrected strain–stress ($\varepsilon_p^c - \sigma$) graphs of the miniature specimens and the strain–stress ($\varepsilon_p^s - \sigma$) graphs of the standard specimens are in good agreement and both miniature and standard geometries show the same elastic slope.

For each type of steel, elastic slope of the standard specimens (E^s) were measured from standard elastic strain–stress curves and presented in Table 2. Also, apparent elastic slope (E^{app}), reference elastic slope (E^{ref}) and corrected elastic slope (E^c) of the miniature specimens were determined from apparent elastic strain–stress curves, reference elastic strain–stress curves and corrected elastic strain–stress curves, respectively (Table 2). The relative error of apparent elastic slope (η^{app}) and corrected elastic slope (η^c) were calculated based on the elastic slope of the standard specimens. Although the relative error of apparent elastic strain is around 50–96 % the relative error of corrected elastic strain is less than 10 %. These results show that this model can be considered as a reliable method for calculating the elastic strain of the miniature specimens from the crosshead displacement.

Conclusions

Elastic strain measurement of the miniature specimens (via Digital Image Correlation) and the standard specimens, for different types of steels (M1400, DP1000, DP600 and IF), showed that the specimen geometry has insignificant influence on the actual measured elastic strain of the materials. However, measurements recorded with the crosshead displacements on the miniature specimens displayed higher strain as a result of the effect of the elastic strain of the fillet-zones and the machine compliance. In this paper, a mathematical model for the calculation of the elastic strain in the fillet-zones and the machine compliance is proposed, which allowed the calculation of the elastic strain from the crosshead displacements. The mathematical model is experimentally evaluated for miniature specimens from different types of steels and different dimensions. For each type of steels, the calculated elastic strain and the strain measured on the standard specimens are in good agreement and consequently the proposed model can be used for calculating the elastic strain of the miniature specimens from the crosshead displacement.

Acknowledgments This research was carried out under the project number M41.10.11437 in the framework of the Research Program of the Materials innovation institute M2i (www.m2i.nl). The support of Tata Steel RD&T to this project is acknowledged.

References

1. Valiev RZ, Sergueeva AV, Mukherjee AK (2003) The effect of annealing on tensile deformation behavior of nanostructured SPD titanium. *Scripta Mater* 49:669–674
2. Sun X, Soulami A, Choi KS, Guzman O, Chen W (2012) Effects of sample geometry and loading rate on tensile ductility of TRIP800 steel. *Mater Sci Eng, A* 541:1–7
3. Korsunsky AM, Nguyen GD, Kim K (2006) The analysis of deformation size effects using multiple gauge length extensometry and the essential work of rupture concept. *Mater Sci Eng, A* 423:192–198
4. KarisAllen KJ, Matthews JR (1995) Low damping absorbers and the determination of load–displacement data for pre-cracked charpy specimens. *ASTM STP* 1248:232–245
5. Hurchill CB, Shaw JA, Iadicola MA (2009) Tips and tricks for characterizing shape memory alloy wire: part 2—fundamental isothermal responses. *Exp Tech* 33:51–62
6. Zhao YH, Guo YZ, Wei Q, Topping TD, Dangelewicz AM, Zhu YT, Langdon TG, Lavernia EJ (2009) Influence of specimen dimensions and strain measurement methods on tensile stress–strain curves. *Mater Sci Eng, A* 525:68–77
7. Sergueeva AV, Zhou J, Meacham BE, Branagan DJ (2009) Gage length and sample size effect on measured properties during tensile testing. *Mater Sci Eng, A* 526:79–83
8. Koubaa S, Othman R, Zouari B, El-Borgi S (2011) Finite-element analysis of errors on stress and strain measurements in dynamic tensile testing of low-ductile materials. *Comput Struct* 89:78–90
9. KarisAllen KJ, Morrison J (1989) The determination of instrumented impact machine compliance using unloading displacement analysis. *Exp Mech* 29:152–156

10. Meier ML, Mukherjee AK (2002) The onset of tensile instability. NASA conference publication
11. Kalidindi SR, Abusafieh A, El-Danaf E (1997) Accurate characterization of machine compliance for simple compression testing. *Expl Mech* 37:210–215
12. Pierron ON, Koss DA, Motta AT (2003) Tensile specimen geometry and the constitutive behavior of Zircaloy-4. *J Nucl Mater* 312:257–261
13. Maringa M (2004) Dimensioning of dog bone specimens and numerical analysis of the effects of different fillet radii, clamp area and pinhole loading on the stresses in such specimens. *Afr J Sci Technol Sci Eng Ser* 5:60–72
14. Hajy Akbary F, Santofimia MJ, Sietsma J (2012) Specimen size effects on the tensile behavior of various steels. *Proc of the 2nd SSTT International Conference, Ostrava, Czech Republic, 2–4 October*: 233–238
15. Tang Z, Liang J, Xiao Z, Guo C (2012) Large deformation measurement scheme for 3D digital image correlation method. *Opt Las Eng* 50:122–130
16. Cintrón R, Saouma V (2008), *Strain Measurements with the Digital Image Correlation System Vic-2D*. University of Colorado